

## The First Synthesis of $\text{Pb}_{1-x}\text{Mn}_x\text{Se}$ Nanocrystals

Tianhao Ji, Wen-Bin Jian, and Jiye Fang\*

Department of Chemistry and Advanced Materials Research Institute, University of New Orleans,  
New Orleans, Louisiana 70148

Received March 15, 2003; E-mail: jfang1@uno.edu

Diluted magnetic semiconductors (DMS) have received strong attention due to their application in magneto-optics,<sup>1</sup> spintronics,<sup>2</sup> displays, and lasers.<sup>3</sup> Recently, it has been realized that the magnetic exchange properties of  $\text{Mn}^{2+}$ ,  $\text{Eu}^{3+}$ , and  $\text{Co}^{2+}$  in semiconductor nanocrystals (NCs) can be changed due to the quantum confinement effects.<sup>4</sup> These DMS NCs can be used to investigate and manipulate a single spin (or a small number of spins) that is embedded in a semiconductor quantum dot.<sup>5</sup> Although a number of nanoscaled DMS systems such as  $\text{Cd}_{(1-x)}\text{Co}_x\text{Se}$ ,<sup>6</sup>  $\text{Zn}_{(1-x)}\text{Mn}_x\text{Se}$ ,<sup>7</sup> and  $\text{Cd}_{(1-x)}\text{Mn}_x\text{Se}$ <sup>8</sup> have been thoroughly studied, we have noted that the investigation of DMS NCs is still limited to II–VI and III–V semiconductor systems. Since its exciton Bohr radius is as large as 46 nm,<sup>9</sup> nanometer-sized lead selenide (PbSe), as a IV–VI semiconductor, offers unique access to the regime of large quantum confinement that is hard to detect in either II–VI or III–V materials.<sup>10</sup> Although monodisperse PbSe NCs have recently been synthesized<sup>11</sup> and their optical properties have been studied,<sup>11,12</sup> to our knowledge, an investigation of Mn-doped PbSe ( $\text{Pb}_{1-x}\text{Mn}_x\text{Se}$ ) NCs has not yet been reported. As strong *sp*–*d* exchange coupling exists between the localized moment of the Mn dopant and the band electrons of PbSe,  $\text{Pb}_{1-x}\text{Mn}_x\text{Se}$  NCs may show unique properties which are different from those of the pure PbSe NCs<sup>13</sup> and should be a promising material for spin applications. We have therefore focused our interest on the investigation of  $\text{Pb}_{1-x}\text{Mn}_x\text{Se}$  NCs. In this communication, we report our recent success in the preparation and the analyses of this material.

The challenge in this synthesis is to make sure that the  $\text{Mn}^{2+}$  ions are indeed incorporated into PbSe NCs. Due to the low quality of the Mn-doped sample when being prepared at room temperature<sup>7</sup> and the problem of Mn segregation onto the particle surface even at high temperature<sup>8</sup> when using regular acetate precursors (for  $\text{Pb}^{2+}$  and  $\text{Mn}^{2+}$ ), we have to alternatively employ a special prebonded Se–Mn complex in which the existing Se–Mn bond may assist in “dragging” the  $\text{Mn}^{2+}$  into the PbSe lattice. Previously,  $\text{Mn}_2(\mu\text{-SeMe})_2(\text{CO})_8$  as an ideal Se–Mn-containing precursor has been selected by Mikulec et al.<sup>8</sup> when successfully synthesizing Mn-doped CdSe NCs. We accordingly adopted their choice to use a small amount of  $\text{Mn}_2(\mu\text{-SeMe})_2(\text{CO})_8$  as a source of  $\text{Mn}^{2+}$  and conduct the synthesis at high temperature to enhance the magnitude of the doping level and to minimize the degree of lattice mismatch. In a typical experiment, organometallic precursors [2 mg of  $\text{Mn}_2(\mu\text{-SeMe})_2(\text{CO})_8$  (the preparation method was referred to ref 8), 0.5 mL of 1 M lead (II) 2-ethylhexanoate (Alfa Aesar) which was predissolved in trioctylphosphine (TOP, Aldrich, 90%), and 0.7 mL of Se-TOP solution (1 M for Se)] were premixed with an additional 3 mL of TOP. The mixed solution was rapidly injected into 20 g of trioctylphosphine oxide (TOPO, Aldrich, 90%) with 0.5 mL of oleic acid (Aldrich, 90%) which was heated to 260 °C under an argon stream on a Schlenk line. The hot mixture was vigorously agitated at 260 °C for 1–10 min to produce different average-sized crystals. The crystalline growth was subsequently terminated by

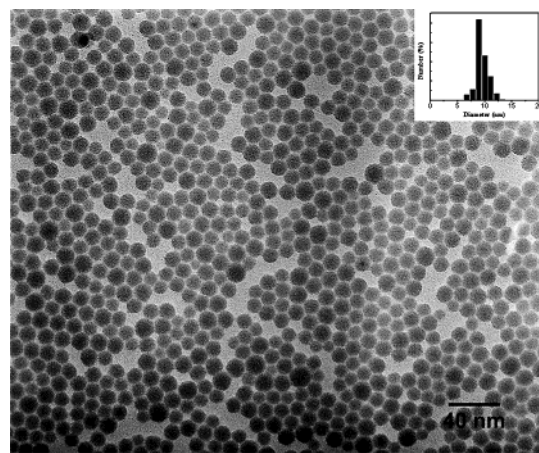


**Figure 1.** TEM image showing the morphology of  $\text{Pb}_{0.985}\text{Mn}_{0.015}\text{Se}$  NCs. The standard deviation of crystalline size was calculated as  $\delta \leq 8\%$ .

cooling it to room-temperature once the dispersion reached the desired size.  $\text{Pb}_{1-x}\text{Mn}_x\text{Se}$  NCs were separated from the multidisperse mixture by a size-selective precipitation, i.e. by centrifugation using a pair of solvents consisting of methanol and toluene. To efficiently eliminate those Mn ions which may physically be adsorbed on the surface of NCs, the as-prepared  $\text{Pb}_{1-x}\text{Mn}_x\text{Se}$  NCs were subsequently immersed into pyridine for 3 days with the assistance of ultrasonics several times (5 min at each time) to perform the ligand exchange on the surface of the size-selected NCs.<sup>14</sup> After the pyridine treatment, the Mn concentration in 10.5 nm NCs was examined by energy dispersive spectroscopy (EDS) and inductively coupled plasma (ICP). We found a strong linear dependence between the EDS or ICP results and input concentrations of the Mn precursor as illustrated in the Supporting Information (Figure S1), indicating the presence of  $\text{Mn}^{2+}$  inside PbSe NCs. The ICP/EDS values will be used for all the further investigations. Figure 1 shows a transmission electron microscopic (TEM) image of the sample  $\text{Pb}_{0.985}\text{Mn}_{0.015}\text{Se}$ , demonstrating a short-range close-packed pattern. The Mn concentration of this sample was determined to be 1.5 mol % (EDS), and the mean crystalline size was measured as 10.5 nm with a standard deviation  $\delta \leq 8\%$ .

To differentiate whether the doped Mn ions are on the surface or in the PbSe NCs, we first measured the lattice constant using X-ray diffraction (XRD). A plot of the lattice parameter (*a*) vs molar percentage of  $\text{Mn}^{2+}$  together with a typical TEM diffraction pattern is shown in Figure 2. The recorded XRD patterns are provided in Figure S2 (Supporting Information). All the detectable peaks are indexed to almost the same positions as those from a standard bulk<sup>15</sup> and from cubic PbSe NCs,<sup>11</sup> but the measured lattice constant is different. We applied Cohen’s method<sup>16</sup> to estimate the average lattice constant (*a*) mainly from the three selected XRD peaks (111), (200), and (220). We found a lattice contraction after introduction of Mn ions. For example, *a* is 6.107 Å for our  $\text{Pb}_{0.990}\text{Mn}_{0.010}\text{Se}$

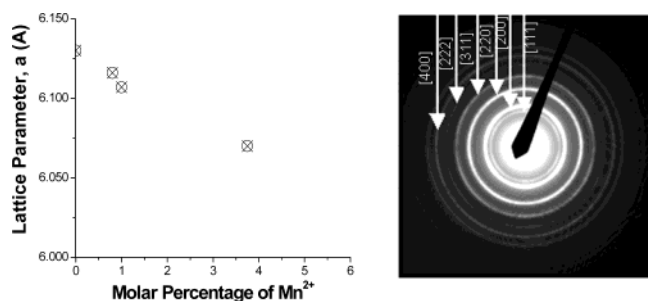


**Figure 2.** (Left) Plot of the lattice parameter,  $a$ , vs molar percentage of  $\text{Mn}^{2+}$ . (Right) Diffraction patterns of  $\text{Pb}_{0.985}\text{Mn}_{0.015}\text{Se}$  (NC size: 10.5 nm).

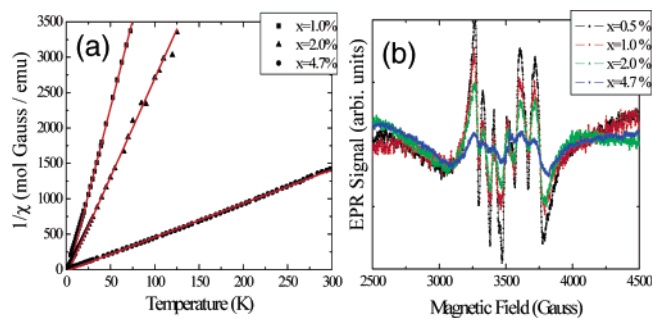


**Figure 3.** (a) Inverse susceptibility of  $\text{Pb}_{1-x}\text{Mn}_x\text{Se}$  NCs measured by SQUID at a field of 10000 Gauss, displaying linear dependence on temperature. The slope of each line is inversely depending on Mn concentration. (b) EPR spectra carried out in an  $x$ -band at room temperature showing that the intensity of hyperfine splittings is variable depending on the Mn concentration.

NCs, compared to 6.130 Å for a pure PbSe NCs (10 nm) which we prepared. We therefore believe that the Mn ions are distributed inside the NCs rather than on the surface, since the substitution of  $\text{Pb}^{2+}$  by  $\text{Mn}^{2+}$  ions may cause some stress and strain effects to shrink the lattice structure. On the basis of the line broadening at half-maximum of the peaks (200) and (220) according to Scherrer equation, the average crystalline size estimated is close to that from our TEM observation. From the XRD results we also found that there is neither  $\text{MnSe}_2$  nor  $\alpha\text{-MnSe}^{17}$  structural phase in our  $\text{Pb}_{1-x}\text{Mn}_x\text{Se}$  samples.

To ensure that the Mn ions are really introduced into the PbSe NCs, we further performed magnetic measurements by a superconducting quantum interference device (SQUID). The PbSe semiconductor is a diamagnetic material confirmed by SQUID results of our pure PbSe NCs (10 nm) (Figure S3 in the Supporting Information). When we doped the NCs with  $\text{Mn}^{2+}$  ions, their magnetic properties dramatically changed from diamagnetic (negative magnetization) into paramagnetic (positive magnetization) behavior. The paramagnetic property displaying a linear dependence between inverse susceptibility ( $1/\chi$ ) and temperature ( $T$ ) is shown in Figure 3a. The slope of each line, which is relative to magnetic moments per NC, does change with increasing of the Mn concentration. We fitted it with the Curie–Weiss law to confirm the Mn concentration inside the PbSe NCs. The fitted concentration of our  $\text{Pb}_{0.953}\text{Mn}_{0.047}\text{Se}$  sample is 0.0481, and the fitted Weiss temperature is 4.36 K. The Weiss temperatures for all of our samples are in the range of 3–5 K which agrees well with a previous result of bulk samples.<sup>18</sup>

In Figure 3b we show the intensity dependence of hyperfine splitting on Mn-concentration carried out by electron paramagnetic resonance (EPR). Each EPR spectrum displays a superposition of a broad curve and six lines of sharp splittings (Figure S4 in Supporting Information). The broad curve is due to electron's spin–spin interactions ( $1/2 \rightarrow -1/2$ ) of isolated Mn ions in the  $\text{Pb}_{1-x}\text{Mn}_x\text{Se}$

NCs, whereas the sharp splitting lines (hyperfine splittings) are due to spin–nucleus interactions. A symmetric Lorentzian line of the broad curve is observed since the sample size is smaller than the skin depth. The nuclear spin of Mn ions is  $5/2$ ; therefore, six hyperfine splittings are observed in the EPR spectra. Hyperfine splitting spectra of various Mn-concentrations were obtained by a subtraction of spin–spin interaction after it was normalized<sup>19</sup> (as shown in Figure 3b). This hyperfine structure shows the electron spin–nuclear spin interactions in an isolated Mn ion. As the Mn ion is affected by other Mn ions that are randomly distributed around it, the Mn–Mn interactions should result in a reduction of the electron spin–nuclear spin interactions in an individual Mn ion. We did observe that the intensity of the spin–nucleus interactions decreases with an increase of Mn concentration. The result confirms again that the Mn ions are embedded in the lattice of our PbSe NC samples.

In summary, we have, for the first time, synthesized Mn-doped PbSe NCs. The existence of  $\text{Mn}^{2+}$  inside the PbSe NCs has been clearly demonstrated by the X-ray diffraction, SQUID, and EPR characterizations. Further investigation on these DMS NCs is significant in the spin applications, such as quantum computing.

**Acknowledgment.** This work was supported by the Office of Naval Research under Grant N00014-02-1-0729 and ARO. We also thank Prieur Elie and Poncho De Leon for their help in conducting ICP analysis and polishing the context, respectively.

**Supporting Information Available:** EDS/ICP results, XRD patterns, SQUID data and EPR spectra. These materials are available free of charge via the Internet at <http://pubs.acs.org>.

## References

- Gorska, M.; Anderson, J. R. *Phys. Rev. B* **1988**, *38*, 9120–9126.
- Wolf, S. A.; Awschalom, D. D.; Buhrman, R. A.; Daughton, J. M.; Molnar, S.; von Roukes, M. L.; Chtchelkanova, A. Y.; Treger, D. M. *Science* **2001**, *294*, 1488–1495; Fiederling, R., Keim M., Reuscher G., Ossau W., Schmidt G., Waag A., Molenkamp L. W. *Nature* (London) **1999**, *402*, 787–790; Ohno H. *Science* **1998**, *281*, 951–956.
- Bhargava R. N. *J. Lumin.* **1996**, *70*, 85–94.
- Raola, O. E.; Strouse, G. F. *Nano Lett.* **2002**, *12*, 1443–1447.
- Gupta, J. A.; Awschalom, D. D.; Peng, X.; Alivisatos A. P. *Phys. Rev. B* **1999**, *59*, R10421–R10424.
- Hanif, K. M.; Meulenber, R. W.; Strouse, G. F. *J. Am. Chem. Soc.* **2002**, *124*, 11495–11502.
- Norris, D. J.; Yao, N.; Charnock, F. T.; Kennedy, T. A. *Nano Lett.* **2001**, *1*, 3–7.
- Mikulec, F. V.; Kuno, M.; Bennati, M.; Hall, D. A.; Griffin, R. G.; Bawendi, M. G. *J. Am. Chem. Soc.* **2000**, *122*, 2532–2540.
- Lipovskii, A.; Kolobkova, E.; Petrikov, V.; Kang, I.; Olkhovets, A.; Krauss, T.; Thomas, M.; Silcox, J.; Wise, F.; Shen, Q.; Kycia, S. *Appl. Phys. Lett.* **1997**, *71*, 3406–3408.
- Wise, F. W. *Acc. Chem. Res.* **2000**, *33*, 773–771.
- Murray, C. B.; Sun, S.; Gaschler, W.; Doyle, H.; Betley, T. A.; Kagan, C. R. *IBM J. Res. Dev.* **2001**, *45*, 47–56.
- Du, H.; Chen, C.; Krishnan, R.; Krauss, T. D.; Harbold, J. M.; Wise, F. W.; Thomas, M. G.; Silcox, J. *Nano Lett.* **2002**, *2*, 1321–1324.
- Kanemitsu, Y.; Matsubara, H.; White, C. W. *Appl. Phys. Lett.* **2002**, *81*, 535–537.
- Kuno, M.; Lee, J. K.; Dabbousi, B. O.; Mikulec, F. V.; Bawendi, M. G. *J. Chem. Phys.* **1997**, *106*, 9869–9882.
- JCPDS-ICDD card 06-0354.
- Cullity B. D., *Elements of X-ray Diffraction*, 2nd ed.; Addison-Wesley Publishing Company Inc.: Reading, Massachusetts, 1978. pp 363–364.
- Peng, Q.; Dong, Y.; Deng, Z.; Kou, H.; Gao, S.; Li, Y. *J. Phys. Chem. B* **2002**, *106*, 9261–9265.
- Górska, M.; Anderson, J. R. *Phys. Rev. B* **1988**, *38*, 9120–9121.
- Felton, N.; Levy, L.; Ingert, D.; Pileni, M. P. *J. Phys. Chem. B* **1999**, *103*, 4–10.

JA0351746